CHEMISTRY
A European Journal

A Journal of
ChemPubSoc Europe

Accepted Article

Title: 1,5-Disubstituted 1,2,3-Triazole-Containing Peptidotriazolamers: Design Principles for a Class of Versatile Peptidomimetics

Authors: Oliver Kracker, Jerzy Góra, Joanna Krzciuk-Gula, Antoine Marion, Beate Neumann, Hans-Georg Stammler, Anke Nieß, Iris Antes, Rafal Latajka, and Norbert Sewald

To be cited as: *Chem. Eur. J.* 10.1002/chem.201704583

Link to VoR: http://dx.doi.org/10.1002/chem.201704583

Supported by
ACES

WILEY-VCH

10.1002/chem.201704583

WILEY-VCH

1,5-Disubstituted 1,2,3-Triazole-Containing Peptidotriazolamers: Design Principles for a Class of Versatile Peptidomimetics

Oliver Kracker,[a] Jerzy Góra,[a],[d] Joanna Krzciuk-Gula,[a],[d] Antoine Marion,[c] Beate Neumann,[b] Hans-Georg Stammler,[b] Anke Nieß,[a] Iris Antes,[c] Rafał Latajka,[d] and Norbert Sewald*[a]

Abstract: Peptidotriazolamers are hybrid foldamers combining features of peptides and triazolamers – repetitive peptidomimetic structures with triazoles replacing peptide bonds. We report on the synthesis of a new class of peptidomimetics, containing 1,5-disubstituted 1,2,3-triazoles in an alternating fashion with amide bonds and the analysis of their conformation in solid state and solution. Homo- or heterochiral peptidotriazolamers were obtained from enantiomerically pure propargylamines with stereogenic centers in the propargylic position and α-azido esters by ruthenium-catalyzed azide-alkyne cycloaddition (RuAAC) under microwave conditions in high yields. With such building blocks the peptidotriazolamers are readily available by solution phase synthesis. While the conformation of the homochiral peptidotriazolamer Boc-Ala*[5Tz]*Phe-Val*[5Tz]*Ala-Leu*[5Tz]*Val-OBzl resembles that of a β VIa1 turn, the heterochiral peptidotriazolamer Boc-D-Ala*[5Tz]*Phe-D-Val*[5Tz]*Ala-D-Leu*[5Tz]*Val-OBzl adopts a polyproline-like repetitive structure.

Introduction

Discrete stable conformations are prerequisites of functional biopolymers, e.g., proteins. Many unique functions of peptides and proteins, including molecular recognition, rely on the prevalence of secondary and/or tertiary structures. Foldamers, a term coined by Gellman,[1] are repetitive structures of naturally occurring or synthetic building blocks that emerged as analogues or surrogates of native biomolecules. They were in many cases proven to be functional biomimetic devices.[2,3]
Hirschmann and co-workers presented in 1992 the novel class of oligopyrrolinones as β-strand peptidomimetics. They contain a strongly modified peptide backbone integrated in cyclic structures also featuring vinylogous amino acids (Figure 1).[4] Similar oligomers composed of 1,4-disubstituted triazoles were described by Arora *et al*. as being reminiscent of a peptide β-strand conformation.[5-7] These triazolamers are somewhat unique as they connect a series of triazole rings by single C_1 units that, at the same time, is a stereogenic centre (Figure 1).

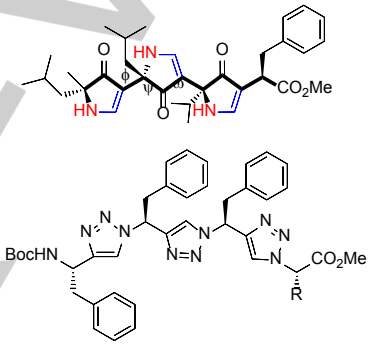

Figure 1. Examples of peptidomimetics: oligopyrrolinones[4] (top) and 1,4-disubstituted triazolamers (bottom).[5-7].

The synthesis of triazoles by thermal 1,3-dipolar cycloaddition of alkynes and azides was first described by Michael *et al*.[8] and later studied systematically by Huisgen.[9] The thermal reaction, e.g., between phenylazide and phenylacetylene, gives a nearly equimolar mixture of the 1,4- and 1,5-disubstituted diphenyltriazole. The copper(I) catalysed azide-alkyne cycloaddition (CuAAC), which was described independently by the groups of Meldal[10] and Sharpless[11] in 2002, exclusively leads to 1,4-disubstituted 1,2,3-triazoles. The CuAAC can be performed either in solution or on solid phase, and has found widespread application.[12-15] This is mainly due to the key features of this versatile reaction: i.e., the reaction proceeds very selectively and without side products in organic or in aqueous media, and is orthogonal towards biologically relevant functional groups. Because of its perfect atom economy and straightforward workup, Sharpless and co-workers considered the CuAAC as a prototype of a "click-reaction".[13] In 2005 its counterpart, the ruthenium(II)-catalysed-azide alkyne-cycloaddition (RuAAC) was presented.[16] In the presence of Cp*RuCl(L_2) the 1,5-disubstituted 1,2,3-triazoles are formed. Although the RuAAC does not tolerate water or protic solvents, it is quite tolerant towards functional groups like alcohols, aldehydes, alkenes, amides, amines, boronic esters, ketones and halides.[17]
Triazoles are considered peptide bond surrogates in peptidomimetics and to be suitable substitutes for amide bonds

[a] O. Kracker, J. Góra, Dr. J. Krzciuk-Gula, A. Nieß, Prof. Dr. N. Sewald*
Organic and Bioorganic Chemistry, Department of Chemistry
Bielefeld University
PO Box 100131, D-33501 Bielefeld, Germany
E-mail: norbert.sewald@uni-bielefeld.de

[b] B. Neumann, Dr. H.-G. Stammler
Inorganic and Structural Chemistry, Department of Chemistry
Bielefeld University
PO Box 100131, D-33501 Bielefeld, Germany

[c] Dr. A. Marion, Prof. Dr. I. Antes
Center for Integrated Protein Science, Department of Biosciences
TU Munich
Emil-Erlenmeyer-Forum 8, D-85354 Freising, Germany

[d] J. Góra, Dr. J. Krzciuk-Gula, Prof. Dr. R. Latajka
Department of Bioorganic Chemistry
Wrocław University of Science and Technology
Wybrzeze Wyspianskiego 27, PL-50-370 Wrocław, Poland

Supporting information for this article is given via a link at the end of the document.

(Figure 2).[18,19] Just like amide bonds, they are planar, have a strong dipole moment and are capable of accepting *H*-bonds. Additionally, they are proteolytically and metabolically stable. While the 1,5-disubstituted triazoles closely resemble a *cis*-configured peptide bond, the 1,4-disubstituted triazole does not perfectly match a *trans*-configured peptide bond.

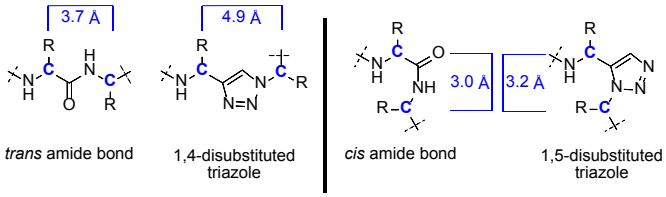

Figure 2. Comparison between *trans*- and *cis*-peptide bonds and their triazole analogues.[20]

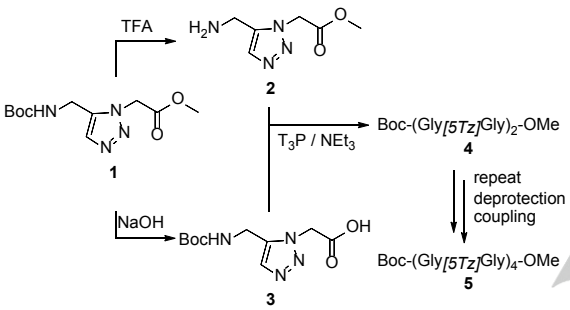

Scheme 1. Building block approach for the synthesis of a glycine-based peptidotriazolamer.

In 2014, Johansson *et al.* published the synthesis of achiral peptidomimetic foldamers containing 1,5-disubstituted 1,2,3-triazoles and amide bonds in an alternating fashion (Scheme 1).[21] As the triazole is considered a peptide bond surrogate, we suggest to adapt the peptidomimetics nomenclature accordingly: If the amide bond -(C=O)-NH- in the dipeptide -Gly-Gly- is replaced by a 1,5-disubstituted triazole it is represented by -Gly*[5Tz]*Gly-.

Because of the polarity of the triazole units and amide bonds, these oligomers are water soluble with the solubility slightly increasing with chain length. Conformational analysis of the oligomers and quantum chemical calculations revealed the co-existence of several conformers with comparable stabilities.[21] Based on the fact that achiral monomers were used, the secondary structure motifs are independent on different side chains and rather formed by backbone interactions.

Triazoles substituted with adjacent stereogenic centres require enantiomerically pure propargylamines and α-azido acids. The synthesis of chiral propargylamines **9** has been described using protected α-amino aldehydes **7** in a Corey-Fuchs or Bestmann-Ohira reaction (Scheme 2).[22-24] The α-amino aldehydes are accessible by either reduction of the corresponding Weinreb amide, by $LiAlH_4$/DIBAL-H, or oxidation of the amino alcohol by Swern oxidation.[25] However, these α-amino aldehydes are very prone to epimerization during prolonged storage or upon contact with silica and are, therefore, to be used immediately.

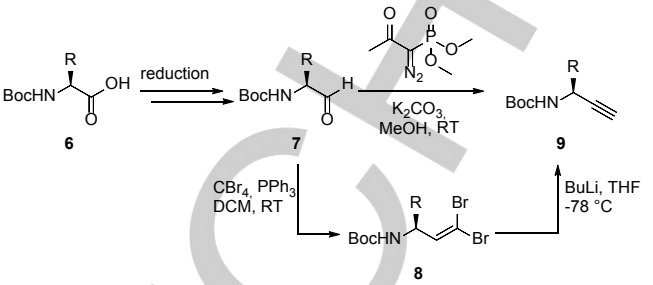

Scheme 2. Synthesis of chiral propargylamines by the Corey-Fuchs or Bestmann-Ohira reaction.

While several protocols for the synthesis of chiral propargylamines have been published, most of these publications are solely comparing the optical rotation of the final product. Recent publications reported partial epimerization upon reaction of the Bestmann-Ohira reagent with chiral α-amino aldehydes.[26-28] The risk of epimerization at the aldehyde stage is increased when electron withdrawing sidechain residues are present that further increase the acidity in α-position to the carbonyl group. Recrystallization of a partially epimerised *N*-protected chiral propargylamine was shown to increase the enantiomeric excess.[29]

Both methods rely on the natural chiral pool. In addition, robust methodology for the synthesis of chiral propargylamines with non-natural side chain residues is available with Ellman's *tert*-butylsulfinamide as a chiral auxiliary (Scheme 3).[30-33] This auxiliary reacts with aldehydes in a condensation reaction to form *N*-sufinyl aldimines **10**, which are further converted by organometallic reagents **11** to give chiral amines **12**.

The *N*-sulfinyl group can be cleaved under acidic conditions to release the free amine as a salt. Hence, the *N*-sulfinyl group has been suggested to be used as a protecting group similar to the Boc group. Moreover, after acidic cleavage, it was shown that the auxiliary can be recovered from the reaction.[34,35]

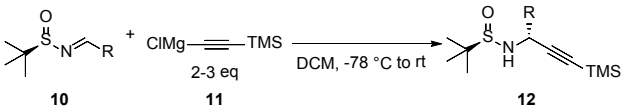

Scheme 3. Diastereoselective synthesis of chiral *N*-sulfinyl propargylamines (R= ^{i}Pr, tBu, $CH_2OTBDPS$), Ph, p-Cl-Ph, p-NO_2-Ph, p-MeO-Ph, thienyl, furyl, Boc-pyrrolyl.[30-33]

Foldamers composed from building blocks presenting amino acid side chains and able to adopt a regular and predictable conformation have potential for controlling protein-protein interaction and peptide aggregation.[1-3]

Results and Discussion

We embarked on a bottom-up approach investigating the conformational behaviour of homo- (**13**) or heterochiral (**14**) peptidotriazolamers as modulators of protein-protein interaction (Figure 3).

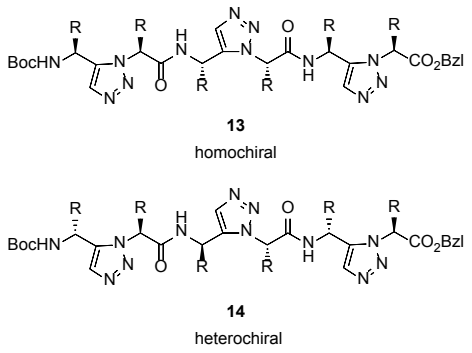

Figure 3. Homochiral and heterochiral peptidotriazole hexamers.

Peptidotriazolamer building blocks of type **20** were synthesized in solution with orthogonal Boc/Bzl protection using triazole derivatives **17**. The *C*-terminal ester is indispensable, since the RuAAC is not compatible with free carboxylic acids (Scheme 4). Such peptidotriazolamers can be synthesized according to a building block approach using triazole derivatives previously synthesized from a propargylamine and an α-azidocarboxylic acid. Alternatively, a submonomer approach involving amide bond formation of an α-azidocarboxylic acid, followed by RuAAC with a protected propargylamine would be feasible.

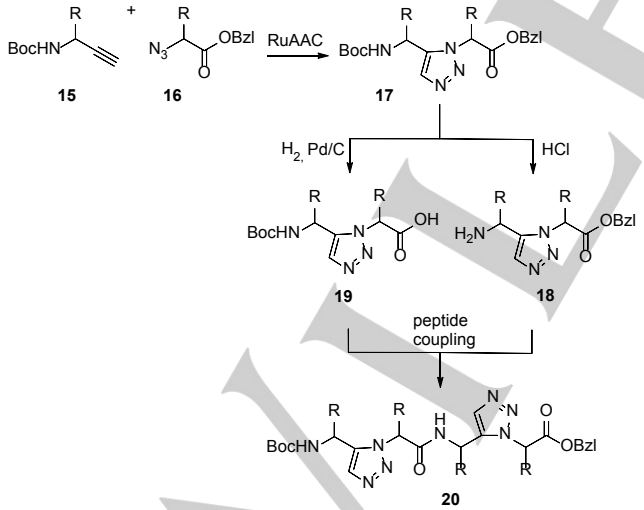

Scheme 4. Envisaged strategy for solution synthesis of peptidotriazolamers using 1,5-disubstituted triazole building blocks obtained by RuAAC.

The synthesis of chiral α-azido esters **22** preferably makes use of the pool of naturally occurring amino acids that can be converted by Cu(II)-catalysed diazo transfer from triflyl azide (Scheme 5).[36,37] By employing Wong's procedure, the azides **22a-c** were synthesized in excellent yields of >87%, starting from commercially available amino acid benzyl ester salts **21**.

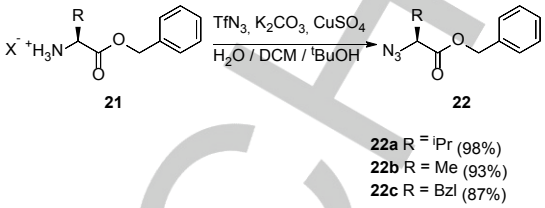

Scheme 5. Synthesis of chiral α-azido esters.

The (*R*) or (*S*) configured propargylamines were obtained using Ellman's auxiliary as described by Wünsch *et al*.[33] Although the *tert*-butylsulfinyl (Bus) group had been previously discussed as a substitute for the Boc group in peptide synthesis, we found it to be unstable under microwave conditions during the RuAAC. Moreover, it decomposes upon standing in polar solvents. A thermal rearrangement of the sulfinamides as investigated by Arava *et al*.[38] was identified to be responsible for low yields in the RuAAC. Accordingly, *N*-sulfinyl propargylamines react intermolecularly forming deprotected and *N*-(*tert*-butylthio)-*tert*-butylsulfonamide linked alkyne. Because of this prominent side reaction, the Bus-protected propargylamines **23** were deprotected (**24**), and the Boc group was introduced (**25**) (Scheme 6).

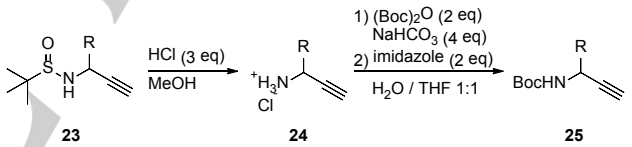

25a R = (S)-Me (61%)
25b R = (R)-Me (85%)
25c R = (S)-^{i}Pr (56%)
25d R = (R)-^{i}Pr (90%)
25e R = (S)-^{i}Bu (82%)
25f R = (R)-^{i}Bu (94%)

Scheme 6. Acidic methanolysis of the Bus group, followed by Boc protection leads to Boc protected propargylamines in good yields over two steps.

Based on a publication by Basel *et al*., imidazole was used to scavenge the slight excess of $(Boc)_2O$, which can be removed by washing with dilute acid, thus avoiding the necessity of a column chromatography in most cases.[39] Using this procedure, the Boc protected (*R*) or (*S*) configured alkyne analogues of Ala (**25a,b**), Val (**25c,d**), and Leu (**25e,f**) were successfully synthesized in enantiomerically pure form.

The RuAAC was performed under microwave conditions. THF turned out to be a suitable solvent, regarding solubility of the starting material, boiling temperature and stability of the catalyst. Noteworthy, additional degassing of freshly destilled THF was not required. Using a slight excess of azide **22**, the RuAAC was complete in 1-2 h providing different homo- and heterochiral triazoles **28-33** representing dipeptide isosters in excellent yields of >80% (Scheme 7).

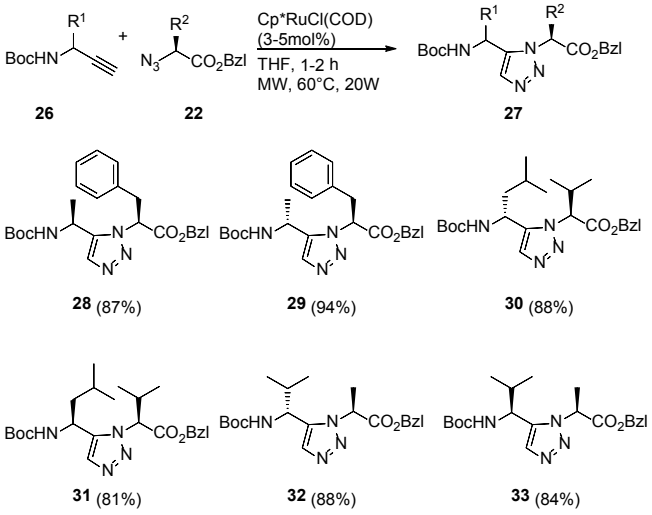

Scheme 7. Microwave-assisted RuAAC providing 1,5-disubstituted triazole building blocks.

The crystallographic data confirm the formation of the 1,5-disubstituted regioisomer in the RuAAC. Moreover, it highlights the turn inducing effect of the 1,5-disubstituted triazole, as shown for Boc-Val*[5Tz]*Ala-OBzl (**33**) as an example, with a distance of 3.17 Å between both α-carbons, displaying close resemblance to a *cis*-peptide bond (Figure 4) (see Supporting Information for additional crystallographic data).

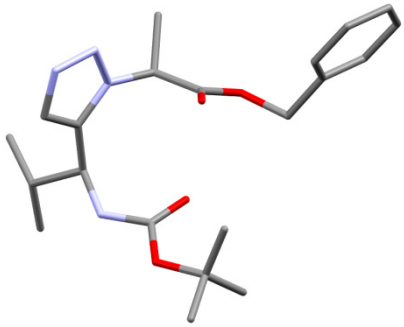

Figure 4. Crystal structure of Boc-Val*[5Tz]*Ala-OBzl (**33**), displaying the chain reversal induced by the 1,5-disubstituted triazole.

With the homo- and heterochiral triazole dipeptide building blocks **28-33** in hand, solution phase peptide synthesis was used for the assembly of larger peptidotriazolamers. The acidic cleavage of the Boc group and hydrogenolysis of the benzyl ester, resp., were quantitative. The deprotected derivatives were used without further purification for the peptide coupling (Schemes 8, 9). With TBTU or HATU as coupling reagents in DMF, either without or in combination with HOBt/HOAt and DIPEA as a base, the products were obtained in high yields, but suffered from epimerization. Carpino and El-Faham had demonstrated the influence of solvent and base on the preactivation rate of amino acids with DIC/HOAt and suggested to use a base-free preactivation in DCM, instead of DMF.[40] The problem of possible epimerization during the coupling of triazole dipeptide-isosteric building blocks was also reported for 1,4-disubstituted triazoles.[41,42] Horne *et al.* overcame this problem by coupling with a five-fold excess of triazole/DIC/HOAt to a free amine on solid phase, without the use of any base for the coupling step.
In our work 2,4,6-trimethylpyridine (*sym*-collidine) was used as a base to liberate the amine from the hydrochloride salt, obtained upon cleavage of the Boc group. The peptide coupling was not accompanied by epimerization at the triazole substituted stereogenic centres when using a base-free, carbodiimide mediated preactivation of the carboxylic acid, in combination with Oxyma-Pure or HOAt, respectively.[43] Hence, a 1.1-fold excess of activated acid, in combination with *sym*-collidine as a base for liberating the amine from the ammonium salt, was sufficient to full conversion of the amine. Under these conditions, coupling proceeded in DCM without any epimerization and with high yields (Schemes 8, 9).

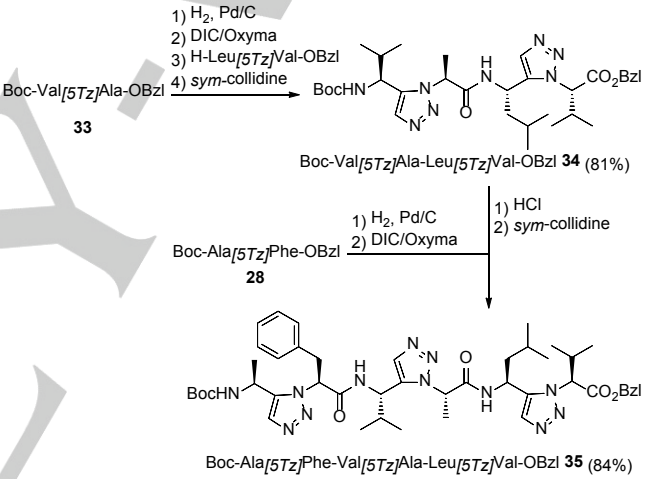

Scheme 8. Synthesis of the hexameric homochiral peptidotriazole **35**.

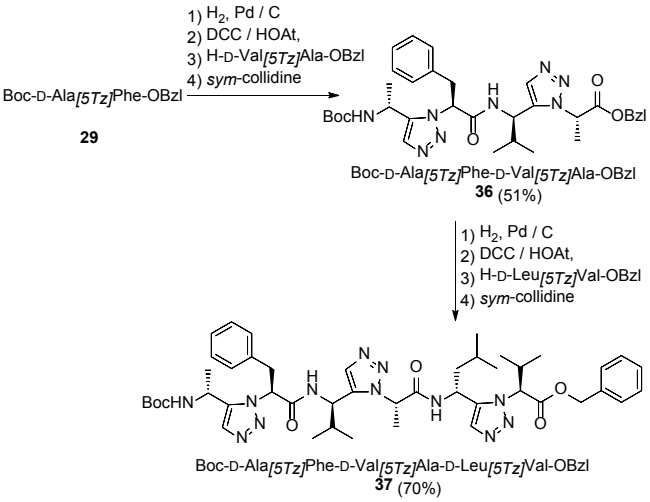

Scheme 9. Synthesis of the hexameric heterochiral peptidotriazole **37**.

The peptidotriazolamers could be purified by either column chromatography or preparative HPLC. In contrast to Johansson *et al.*,[21] a drastic decrease in coupling yields of the tetramer to give the hexamer units was not observed. Furthermore, the carbodiimide mediated coupling provides increased coupling yields, compared to the T_3P/DIPEA system Johansson *et al.* used for their achiral oligomers. If solubility of the hydrochloride salt in DCM becomes a problem, it can be dissolved in DMF and added dropwise to the preactivated acid, dissolved in DCM, for a final DCM/DMF ratio of 1:1 without any epimerization.

Conformational analysis

The X-ray single crystal structure analysis of the tetramer Boc-Val*[5Tz]*Ala-Leu*[5Tz]*Val-OBzl (**34**) revealed the torsion angles of the peptide backbone in the solid state (Figure 5, Table 1). The conformation is being stabilized by an intramolecular hydrogen bond between the Boc carbonyl oxygen and the amide proton of Leu, with a distance of 2.08 Å.

We also modeled the structures of **34**, **35**, and **37** by means of molecular dynamics (MD) simulations to further characterize the conformational preferences of the 1,5-substituted peptidotriazolamers. The simulations were based on the specific TZLff molecular mechanics force-field parametrization of 1,4- and 1,5-substituted triazole-based peptidomimetics that we recently developed.[44] As the backbone of peptidotriazolamers differs from standard polypeptides, we use here the following nomenclature to label the torsion angles: φ_n=$C_{(c=0)}$-$N_{(NH)}$-C_α-C5; ψ_n=$N_{(NH)}$-C_α-C5-N1; φ_c=C_5-N_1-C_α-$C_{(C=O)}$; ψ_c=N_1-C_α-$C_{(C=O)}$-$N_{(NH)}$.

We performed a non-restrained simulated annealing (SA) of peptidotriazolamer **34** in the gas phase to compare the structure with the solid-state structure. The simulation was started from a random conformation of the molecule, far from that of the crystal structure, in order to avoid any bias in our modeling attempt. The final structure is depicted in Figure 5 and the values of backbone torsions are reported in Table 1, along with those of the X-ray analysis. Both structures show a nearly identical backbone conformation, with a bend in the middle of the sequence that is stabilized by an intramolecular hydrogen bond. Further simulations of **34** in DMSO are reported in our previous publication.[44] The agreement between experimental and modeled structures is very good, making us confident about the validity of the next step of this study.

Table 1. Comparison of the torsion angles of the tetramer **34** according to X-ray analysis and molecular dynamics (MD) simulation.

	$\varphi_{n/c}$		$\psi_{n/c}$	
	X-ray	MD	X-ray	MD
Val1	-66.4(2)°	-66.3°	132.8(1)°	130.9°
Ala2	-112.2(2)°	-111.4°	39.8(2)°	30.4°
Leu3	-128.6(1)°	-131.0°	57.7(2)°	57.1°
Val4	-93.2(2)°	-100.4°		

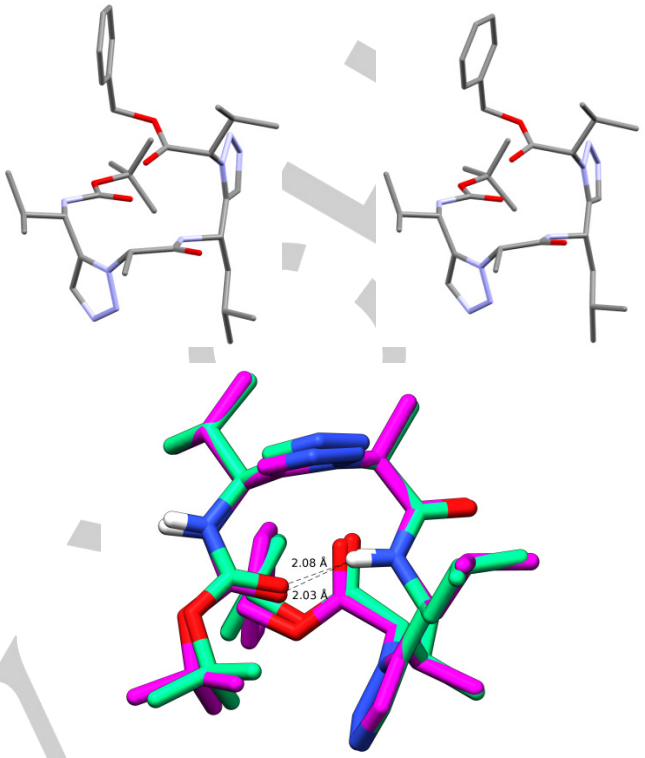

Figure 5. Comparison of solid-state (top, left) and simulated (top, right) conformation of the peptidotriazolamer **34** and an overlay of both structures (bottom; all atoms RMSD = 0.37 Å; green: X-ray; magenta: MD).

For peptidotriazolamers **35** and **37** the first stage of the calculations consisted of NMR data refinement by means of gas-phase simulated annealing followed by an MD simulation in the original NMR solvent (DMSO) with ROESY-derived distance restraints imposed on both calculations. Furthermore, we performed additional unrestrained MD simulations in DMSO and water in order to validate the adequacy of the initial set of distance restraints, sample regions of the conformational space that may have been previously inaccessible and observe the behavior of the analyzed compounds in a different solvent model.

During the distance-restrained MD simulation run the torsional angles of **35** oscillated around the values produced by the SA run (Figure 6A). This indicates that the initial set of NMR-derived distance restraints manages to reproduce the conformational behavior of **35** even without the presence of explicit solvent. At 300 K the system samples a restricted number of conformations, similar to the final structure obtained from SA and has a fairly compact structure (Figures 5A, 7A).

Table 2. Torsion angles for the representative structure of **35** observed during distance-restrained MD in DMSO and water.

	$\varphi_{n/c\ (DMSO)}$	$\psi_{n/c\ (DMSO)}$	$\varphi_{n/c\ (water)}$	$\psi_{n/c\ (water)}$
Ala1	-112.9°	62.8°	-137.2	74.2
Phe2	-92.6°	83.1°	-120.2	7.5
Val3	-61.1°	123.9°	-79.7	116.4
Ala4	-108.5°	52.1°	-100.0	1.9
Leu5	-91.3°	99.2°	-132.4	136.2
Val6	-166.0°	-	-50.0	-

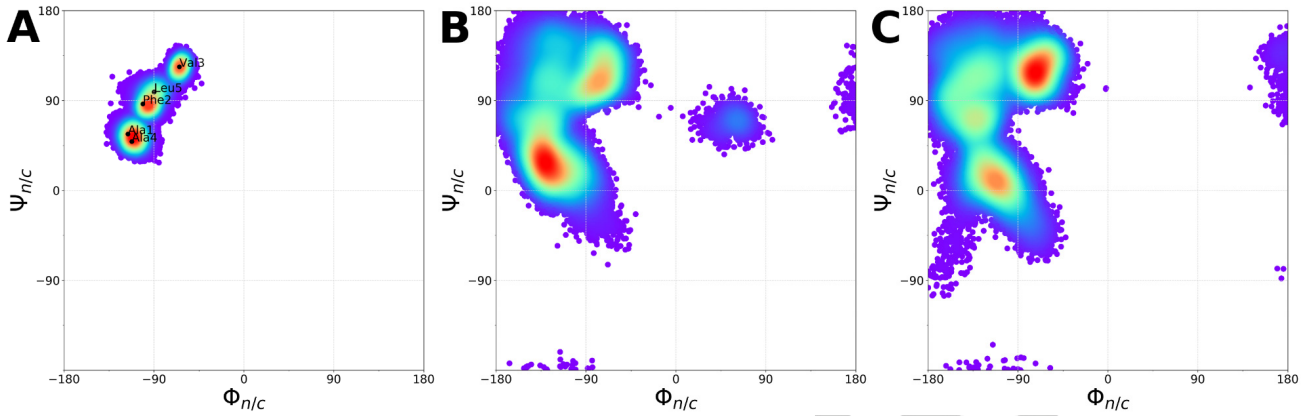

Figure 6. φ/ψ Distribution for **35** during distance-restrained MD in DMSO (**A**; black dots annotate torsional angle values from SA) and unrestrained simulations in DMSO (**B**) and in water (**C**).

The representative conformation from clustering over the last 100 ns of the simulation resembles that of a β-turn for natural peptides. It is stabilized by a well-conserved hydrogen bond (persisting for 91.7% of the clustered trajectory) formed between the i and i+3 residues (Phe2 and Leu5). The corresponding values of torsional angles for the i+1 and i+2 residues (Table 2) suggest that it resembles a type VIa1 β-turn. In this conformation, the backbone of the molecule is folded towards the inner side of the turn, whereas the side chains are protruding towards the solvent. The overall conformation of **35** is also in good agreement with X-ray data obtained for its precursor **34** (Figure 4, Table 1). The torsional angle values are comparable and both compounds form a turn stabilized by an internal hydrogen bond.

The heterochiral peptidotriazolamer **37** displays more flexibility upon sampling of the conformational space in course of the distance-restrained MD simulation (Figure 7A, Table 3). This was an expected result as a lower number of crosspeaks could be observed on the ROESY spectra in comparison to **35**. Accordingly, only a total of 22 distance restraints was generated for **37** in contrast to 55 restraints for **35**. The peptidotriazolamer **37** displayed a tendency to adopt an extended conformation, which allows accessing a wider variety of conformations. This applies predominantly to the side chains and the Boc protecting group, which was not involved in any distance restraint. As a result, two additional basins at (-160°, 160°) and (160°, -160°) of the phi/psi distribution plot can be observed in contrast to the data established during SA.

This highlights the advantage of using an explicit solvent model for the improvement of conformational space sampling, especially in case of extended conformations, where it is likely to observe less cross-peaks on ROESY and NOESY spectra. The representative structure (Figure 9A) is not stabilized by any intramolecular hydrogen bond. The triazole rings are located on the same side of the backbone and are almost stacked upon one another, while the side chains are presented on the opposite site of the structure. The overall fold bears a distant similarity to the polyproline family of helices. It resembles a left-handed helix with no hydrogen bonding and three residues per turn, which are the features of a polyproline helix. It is, however, more denser and contains *cis* peptide bond analogues. Thus, it is reminiscent of the polyproline I type helix.

Subsequently, we performed unrestrained simulations in DMSO to assess a more realistic picture of the dynamics of the two peptidomimetics. As expected, the release of the constraints

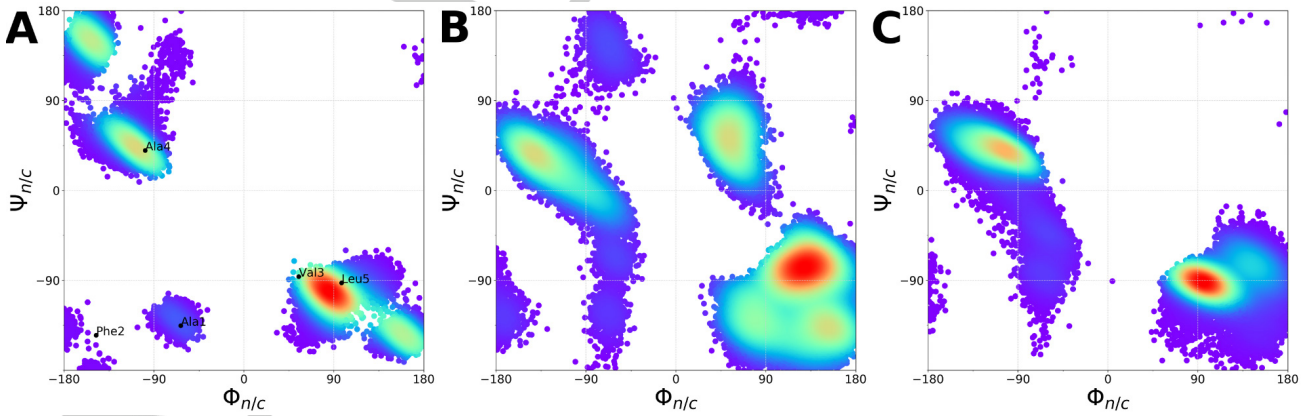

Figure 7. φ/ψ Distribution for 37 during distance-restrained MD in DMSO (**A**; black dots annotate torsional angle values from SA) and unrestrained simulations in DMSO (**B**) and in water (**C**).

resulted in sampling of new regions, which were inaccessible during the previous simulations (Figures 5B, 7B). The effects are more apparent for **37** (Figure 7B) because of its extended conformation and lack of intramolecular stabilization. For both compounds the overall backbone conformation of their representative structures is very similar to the one derived from distance-restrained MD. Two major clusters (45.9% and 25.9% of the clustered population) can be distinguished for **35** (representative structure of dominant cluster, Figure 8B; representatives of the main clusters, Figure SI 23) and three (36.5%, 23.3% and 12.3% of the clustered population) for **37** (representative structure of dominant cluster, Figure 9B; representatives of the main clusters, Figure SI 24). The two conformers of **35** share a similar fold of the backbone with slight variations of the more flexible extremities. In case of **37** a larger fragment of the *N*-terminus, consisting of the Boc protecting group and the first two amino acid residues (Ala1, Phe2) exhibit an increased degree of freedom and fold onto the backbone. In this scenario, there are three distinct positions of the *N*-termini for the conformers of **37**. Therefore, when comparing restrained and conventional MD simulations, an additional basin around (60°, 60°) appears on the φ/ψ distribution plot of the latter (Figure 7B, Table 3). The remaining residues of the molecule adopt a conformation that is well preserved among the representatives of the three clusters.

Table 3. Torsion angles of the representative structure of **37** observed during restrained MD in DMSO and water.

	$\varphi_{n/c\ (DMSO)}$	$\Psi_{n/c\ (DMSO)}$	$\varphi_{n/c\ (water)}$	$\Psi_{n/c\ (water)}$
D-Ala1	145.6	-140.9	163.9	-83.2
Phe2	-135.3	151.8	-130.3	39.2
D-Val3	84.3	-92.3	102.4	-87.9
Ala4	-106.2	43.0	-95.7	39.4
D-Leu5	92.9	-103.3	100.6	-90.4
Val6	-71.9	-	-68.6	-

To gain insights into the behavior of the compounds in a more biological environment, we performed unrestrained MD runs in pure TIP4Pew water.[45] Changing the solvent polarity restricts the conformational space for **35** and **37**. Within the limits of the current simulations, both compounds exhibit a single dominant cluster (**35**: 88.7%; **37**: 84.4%). The structure of **35** remains mostly unchanged compared to its counterpart in DMSO and still resembles a β-turn stabilized by the internal hydrogen bond between Phe2 and Leu5 (Figure 8C, Table 2). On the other hand, the helical shape of **37** appears slightly more pronounced in water (Figure 9C, Table 3) than during the simulation in DMSO.

In Figures SI 25 and SI 26 (see supporting information) we

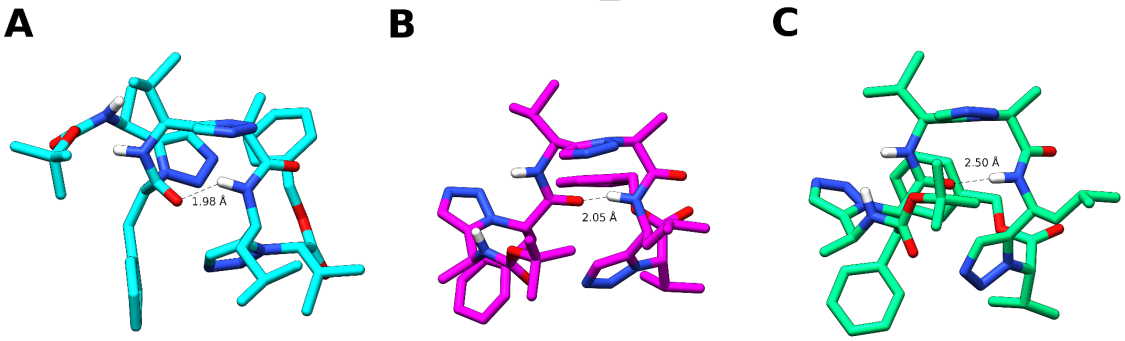

Figure 8. Representative structures for **35** derived from clustering over the last 100 ns of distance-restrained MD in DMSO (**A**) and unrestrained simulations in DMSO (**B**) and in water (**C**).

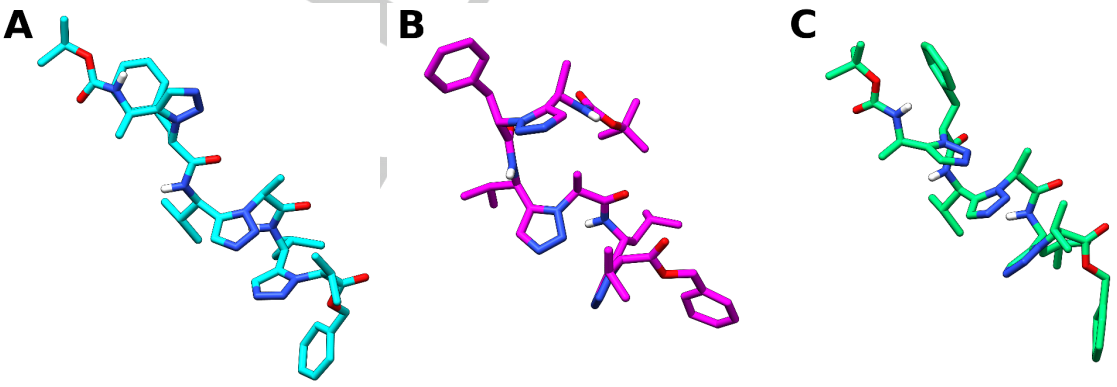

Figure 9. Representative structures for **37** derived from clustering over the last 100 ns of distance-restrained MD in DMSO (**A**) and unrestrained simulations in DMSO (**B**) and TIP4Pew water (**C**).

display the radial distribution functions (RDF) for chosen backbone atoms of **35** and **37**, and Figure 10 highlights the most relevant results. Such analysis reflects the solvation of specific parts of the compounds and allows to further characterize their behavior in water. In general, the plots show little to no structuration of the solvent around the two molecules. Some hydrophilic groups display clear narrow peaks at distances characteristic for hydrogen bonds indicating stable interactions with water. However, the intensity of these peaks is rather small and the second solvation shell is found further away. This shows that the global solvation of the molecules is rather poor, which is in agreement with the hydrophobic character of the side chains. All triazole rings show similar solvation with N2 and N3 acting as hydrogen bond acceptors. The RDFs corresponding to the hydrogen atoms of the rings (H4) show no particular structuration, emphasizing their low electrophilic character, as discussed by Marion *et al*.[44] While most interactions for the two analyzed compounds are matching, a clear difference appears for the solvation of two backbone amino acid, i.e. Phe2 (O) and Leu5 (H). In **35**, the RDFs of both atoms (Figure 10) show that the first accessible water molecules are found at distances greater than 4.0 Å.

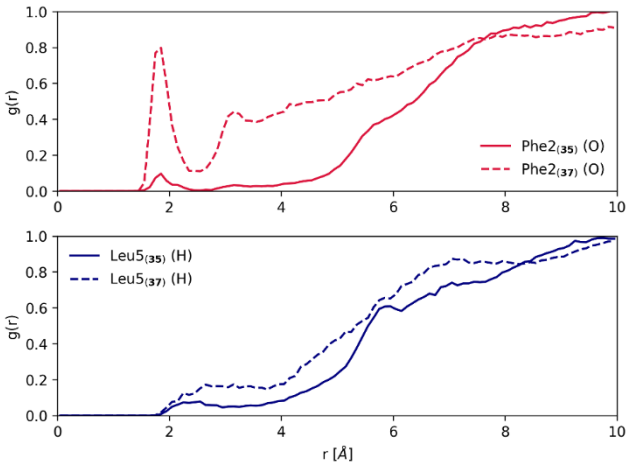

Figure 10. Radial distribution functions for chosen backbone atoms of **35** (top) and **37** (bottom).

This is directly correlated with the fact that these atoms are involved in formation of an intramolecular hydrogen bond, as identified during the clustering analysis. In contrast, the extended conformation of **37** allows better solvation of the backbone in comparison to **35**. In consequence, the RDF of Phe2 (O) of **37** (Figure 10) has a clear narrow peak centered at 1.8 Å. The backbone hydrogen atom Leu5 (H) in **37** is slightly more accessible to water molecules, but does not show any particular structuration, most likely due to large size of the aliphatic side chain of this amino acid. Overall, this analysis shows that the conformational differences between **35** and **37** highlighted during the clustering analysis have an impact on their respective solvation in water. While both compounds show quite poor solvation, the extended conformation of **37** allows for interaction of all backbone hydrophilic groups with water. On the other hand, the compact conformation of **35** increases the hydrophobic character of the molecule.

Conclusions

We have developed an efficient and robust synthesis route leading to conformationally versatile peptidomimetic foldamers, containing chiral 1,5-disubstituted triazoles in an alternating fashion with amide bonds. Peptidomimetics with alternating amide bonds and 1,5-disubstituted triazoles were obtained in a building block approach: Six different homo- and heterochiral building blocks Boc-Xaa*[5Tz]*Yaa-OBzl were synthesized in high yields from chiral propargylamines and α-azido acids by Ruthenium-catalyzed azide-alkyne cycloaddition (RuAAC) under microwave condition. Epimerization during the formation of the peptide bonds could be prevented by a base-free carbodiimide mediated preactivation.
The solid-state conformation of the homochiral tetramer Boc-Val*[5Tz]*Ala-Leu*[5Tz]*Val-OBzl **34** and the structure from simulated annealing in the gas phase without any constraint match very well. The conformational preferences of the peptidotriazolamer hexamers Boc-Ala*[5Tz]*Phe-Val*[5Tz]*Ala-Leu*[5Tz]*Val-OBzl **35** and Boc-D-Ala*[5Tz]*Phe-D-Val*[5Tz]*Ala-D-Leu*[5Tz]*Val-OBzl **37** were elucidated by NMR measurements and MD simulations in DMSO and in water. While the homochiral peptidotriazolamer **35** forms a compact β-turn-like structure, the heterochiral peptidotriazolamer **37** with alternating chirality adopts a polyproline I-like conformation.

Acknowledgements

The authors gratefully acknowledge financial support from Deutsche Forschungsgemeinschaft (DFG), Project SE 609/10-1, Deutscher Akademischer Austauschdienst (DAAD), Project ID 57333947, the Leading National Research Centre (KNOW, Poland), the BioNam: Bionanomaterials project, the Polish Ministry of Science and Higher Education (PMSHE) for the Faculty of Chemistry of Wrocław University of Science and Technology, Wroclaw Centre for Networking and Supercomputing (http://wcss.pl), grant No. 197.

Conflict of Interest

The authors declare no conflict of interest.

Keywords: Peptidomimetics • Foldamers • Peptidotriazolamers • RuAAC • Conformational Analysis

[1] S. H. Gellman, *Acc. Chem. Res.* **1998**, *31*, 173–180.
[2] J. W. Checco, S. H. Gellman, *Curr. Opin. Struct. Biol.* **2016**, *39*, 96–105.
[3] R. Gopalakrishnan, A. I. Frolov, L. Knerr, W. J. Drury III, E. Valeur, *J. Med. Chem.* **2016**, *59*, 9599–9621.

[4] A. B. Smith III, T. P. Keenan, R. C. Holcomb, P. A. Sprengeler, M. C. Guzman, J. L. Wood, P. C. Carroll, R. Hirschmann, *J. Am. Chem. Soc.* **1992**, *114*, 10672–10674.
[5] N. G. Angelo, P. S. Arora, *J. Am. Chem. Soc.* **2005**, *127*, 17134–17135.
[6] N. G. Angelo, P. S. Arora, *J. Org. Chem.* **2007**, *72*, 7963–7967.
[7] A. L. Jochim, S. E. Miller, N. G. Angelo, P. S. Arora, *Bioorg. Med. Chem. Lett.* **2009**, *19*, 6023–6026.
[8] L. I. Smith, *Chem. Rev.* **1938**, *23*, 193–285.
[9] R. Huisgen, *Angew. Chem., Int. Ed.* **1963**, *2*, 565–632.
[10] C. W. Tornøe, C. Christensen, M. Meldal, *J. Org. Chem.* **2002**, *67*, 3057–3064.
[11] V. V. Rostovtsev, L. G. Green, V. V. Fokin, K. B. Sharpless, *Angew. Chem., Int. Ed.* ***2002****, 41, 2596–2599.*
[12] M. Meldal, C. W. Tornøe, *Chem. Rev.* **2008**, *108*, 2952–3015.
[13] H. C. Kolb, K. B. Sharpless, *Drug Discov. Today* **2003**, *24*, 1128–*1137*.
[14] Y. L. Angell, K. Burgess, *Chem. Soc. Rev*. **2007**, *36*, 1674–*1689*.
[15] (a) V. D. Bock, H. Hiemstra, J. H. van Maarseveen, *J. Org. Chem.* **2006**, 51–*68*; (b) K. Nwe, M. W. Brechbiel, *Cancer Biother. Radiopharm.* **2009**, *24*, 289–*302*; (c) C. D. Hein, X. -M. Liu, D. Wang, *Pharm. Res.* **2008**, *25*, 2216–*2230*; (d) G. C. Tron, T. Pirali, R. A. Billington, P. L. Canonico, G. Sorba, A. A. Genazzani, *Med. Res. Rev*. **2008**, *28*, 278–*308*; (e) J. E. Moses, A. D. Moorhouse, *Chem. Soc. Rev.* **2007**, *36*, 1249–1262.
[16] L. Zhang, X. Chen, P. Xue, H. H. Y. Sun, I. D. Williams, K. B. Sharpless, V. V. Fokin, G. Jia, *J. Am. Chem. Soc.* **2005**, *127*, 15998–15999.
[17] B. C. Boren, S. Narayan, L. K. Rasmussen, L. Zhang, H. Zhao, Z. Lin, G. Jia, V. V. Fokin, *J. Am. Chem. Soc.* **2008**, *130*, 8923–8930.
[18] S. G. Agalave, S. R. Maujan, V. S. Pore, *Chem. Asian J.* **2011**, 6, 2696–2718.
[19] D. S. Pedersen, A. Abell, *Eur. J. Org. Chem.* **2011**, 2399–2411.
[20] J. R. Johansson, T. Beke-Somfai, A. S. Stalsmeden, N. Kann, *Chem. Rev*. **2016**, *116*, 14726–14768.
[21] J. R. Johansson, E. Hermansson, B. Nordén, N. Kann, T. Beke-Somfai, *Eur. J. Org. Chem.* **2014**, 2703–2713.
[22] G. Reginato, A. Mordini, F. Messina, A. Degl´Innocenti, G. Poli, *Tetrahedron* **1996**, *52*, 10985–10996
[23] H. D. Dickson, S. C. Smith, K. W. Hinkle, *Tetrahedron Lett.* **2004**, *45*, 5597–5599.
[24] D. Habrant, V. Rauhala, A. M. P. Koskinen, *Chem. Soc. Rev*. **2010**, *39*, 2007–2017.
[25] J. Jurczak, A. Golebiowski, *Chem. Rev.* **1989**, 89, 149–164.
[26] A. Tam, U. Arnold, M. B. Soellner, R. T. Raines, *J. Am. Chem. Soc.* **2007**, *129*, 12670–12671.
[27] E. J. Thomas, M. Willis, *Org. Biomol. Chem.* **2014**, *12*, 7537–7550.
[28] W. Doherty, N. Adler, A. Knox, D. Nolan, J. McGouran, A. N. Nikalje, D. Lokwani, A. Sarkate, P. Evans, *Eur. J. Org. Chem.* **2017**, 175–185.
[29] M. Nahrwold, T. Bogner, S. Eissler, S. Verma, N. Sewald, *Org. Lett.* **2010**, *5*, 1064–1067.
[30] J. A. Ellman, *Pure Appl. Chem.* 2003, *75*, 39–46.
[31] B. C. Chen, B. Wang, G. Q. Lin, *J. Org. Chem.* **2010**, *75*, 941–944.
[32] L. Ye, W. He, L. Zhang, *Angew. Chem., Int. Ed.* **2011**, *50*, 3236 –3239.
[33] M. Wünsch, T. Fröhr, D. Schröder, L. Teichmann, J. Rudlof, P. Holtkamp, S. Heidemeyer, L. Klemme, S. Hedwig, N. G. Janson, A. Hinzmann, J. Simon, C. Belu, B. Neumann, H. -G. Stammler, N. Sewald, *Beilstein J. Org. Chem.* **2017,** *13,* 2428–2441.
[34] M. Wakayama, J. A. Ellman, *J. Org. Chem.* **2009**, *74*, 2646–2650.
[35] M. T. Robak, M. A. Herbage, J. A. Ellman, *Chem. Rev.* **2010**, *110*, 3600–3740.
[36] P. B. Alper, S. C. Hung, C. H. Wong, *Tetrahedron Lett.* **1996**, *37*, 6029–6032.
[37] J. T. Lundquist, J. C. Pelletier, *Org. Lett.* 2001, *3*, 781–783.
[38] V. R. Arava, L. Gorentla, P. K. Dubey, *Beilstein J. Org. Chem.* **2011**, *7*, 9–12.
[39] Y. Basel, A. Hassner, *Synthesis* **2001**, *4*, 550–552.
[40] L. A. Carpino, A. El-Faham, *Tetrahedron* **1999**, *55*, 6813–6830.
[41] W. S. Horne, C. D. Stout, M. R. Ghadiri, *J. Am. Chem. Soc.* **2003**, *125*, 9372–9376.
[42] A. Proteau-Gagné, K. Rochon, M. Roy, P. -J. Albert, B. Guérin, L. Gendron, Y. L. Dory, *Bioorg. Med. Chem. Lett*. **2013**, *23*, 5267–5269.
[43] R. Subirós-Funosas, R. Prohens, R. Barbas, A. El-Faham, F. Albericio, *Chem. Eur. J.* **2009**, 9394–9403.
[44] A. Marion, J. Góra, O. Kracker, T. Fröhr, R. Latajka, N. Sewald, I. Antes, *J. Chem. Inf. Model*. **2017**, DOI: 10.1021/acs.jcim.7b00305.
[45] H. W. Horn, W. C. Swope, J. W. Pitera, J. D. Madura, T. J. Dick, G. L. Hura, T. J. Head-Gordon, *Chem. Phys*. **2004**, *120*, 9665–9678.

10.1002/chem.201704583

WILEY-VCH

FULL PAPER

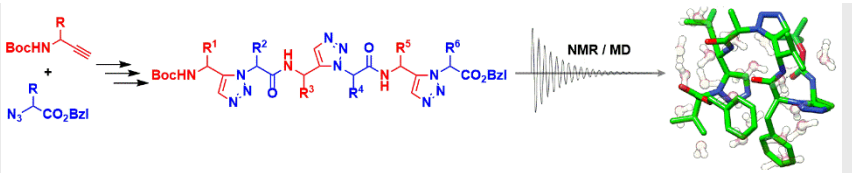

Stereochemistry matters: While the conformation of the homochiral peptidotriazolamer Boc-Ala*[5Tz]*Phe-Val*[5Tz]*Ala-Leu*[5Tz]*Val-OBzl resembles that of a βVIa1 turn, the heterochiral peptidotriazolamer Boc-D-Ala*[5Tz]*Phe-D-Val*[5Tz]*Ala-D-Leu*[5Tz]*Val-OBzl adopts a polyproline-like repetitive structure.

*Oliver Kracker, Jerzy Góra, Joanna Krzciuk-Gula, Antoine Marion, Beate Neumann, Hans-Georg Stammler, Anke Nieß, Iris Antes, Rafał Latajka, and Norbert Sewald**

Page No. – Page No.

Title